ELSEVIER

Journal of Power Sources 102 (2001) 74–81

JOURNAL OF POWER SOURCES

www.elsevier.com/locate/jpowsour

Preliminary experimental and theoretical analysis of limit performance of molten carbonate fuel cells

Elisabetta Arato[a], Barbara Bosio[a,*], Paolo Costa[a], Filippo Parodi[b]

[a]*Department of Environmental Engineering, University of Genova, Via Opera Pia 15, Genova 16145, Italy*
[b]*Ansaldo Ricerche, C.so Perrone 25, Genova 16161, Italy*

Received 31 December 2000; received in revised form 23 March 2001; accepted 27 March 2001

Abstract

The aim of this work is to investigate the limit performance of molten carbonate fuel cells due to gas diffusion phenomena in the porous electrodes when high reactant utilisation factors are used. Modelling and experimental activities are presented. An electrode kinetic micromodel has been performed accounting for the effects of the diffusion limits and has been integrated into a macromodel in order to optimise cell performance and operation. Specific tests have been carried out to identify the dependence of anodic as well as cathodic limiting current density on operating parameters using planar square cells produced by Ansaldo Ricerche (ARI). In turn, limiting current measurements have been used in order to identify overall reactant mass transfer coefficients in the complex structure of the electrodes. A good agreement between simulated and experimental results is presented and discussed.

Keywords: MCFC; Modelling; Diffusion phenomena; Electrode kinetics; Limit performance

1. Introduction

Today one of the most significant sources of pollution is coming from energy/power systems. In this scenario molten carbonate fuel cells (MCFCs) are a promising solution for the production of clean energy with high efficiency and environmental respect, especially for remote users. In particular, MCFC technology is now at the stage of scaling-up to commercialisation and many developers world-wide have shown significant progress.

In order to guide the development process in terms of optimisation of operating conditions and technological solutions, a simulation activity has been carried out and presented in a previous paper [1]: an MCFC macroscopic model has been set-up where a micromodel of the electrode kinetics has been included.

This model has been developed for planar cells with cross-flow gas feeding system. It takes account of mass, energy and momentum balances of the gaseous streams, together with the energy balance of the solid, considering the following chemical and electrochemical reactions:

$$CO_2 + \tfrac{1}{2}O_2 + 2e^- \rightarrow {CO_3}^{2-} \qquad \text{(cathode)}$$

$$H_2 + {CO_3}^{2-} \rightarrow H_2O + CO_2 + 2e^- \qquad \text{(anode)}$$

$$H_2O + CO \rightarrow H_2 + CO_2 \qquad \text{(anode)}$$

The simulation results are available in terms of maps of gas and solid temperatures, electrical current, Nernst voltage, polarisation, internal resistance, pressure drop and composition of the gaseous streams on the cell plane.

The kinetics is expressed as a local electrical resistance function of temperature, pressure, gas composition and phenomenological parameters identified by experimental data. In this way, cell performance is simulated with a linear dependence of cell voltage on current density, obtaining a good agreement between simulation and experimental results when rich reactant feedings are used [1].

However, experimental data collected on MCFC stacks working at high reactant utilisation factors show at high current densities an abrupt voltage drop not foreseen by this micromodel [2]. This trend can be explained in terms of limiting transport phenomena in the porous electrodes, which cause cell voltage decay indicating a limiting current density.

Aim of this paper is to investigate this limit performance of MCFC cells and to extend to a wider operating validity range the electrode kinetics micromodel accounting also for the effects of the diffusion phenomena. For this reason, a number of specific performance curves have been carried out on MCFC cells produced by Ansaldo Ricerche (ARI)

* Corresponding author. Tel.: +39-10-3536507; fax: +39-10-3532589.
E-mail address: bosio@diam.unige.it (B. Bosio).

0378-7753/01/$ – see front matter
PII: S0378-7753(01)00797-2

Nomenclature

A, B, s_{iR}, D, G	parameters in Eq. (2)
c	reactant concentration, mol m^{-3}
E	thermodynamic voltage, V
F	Faraday's constant, C mol^{-1}
J	local current density, A m^{-2}
K_c	mass transport coefficient, m s^{-1}
l	spatial coordinate, m
L	cell length, m
n	number of electrons
p_{O_2}	partial pressure of oxygen, Pa
Q	molar flow-rate for unit length, mol s^{-1} m^{-1}
R	electrical resistance, ohm
R_g	gas constant, J mol^{-1} K^{-1}
T	temperature, K
u	utilisation factor
V	cell voltage, V
y	molar fraction
Greek letters	
β	parameter in Eq. (2)
η_{conc}	concentration polarisation, V
v	stoichiometric coefficient
Superscripts	
b	bulk
0	inlet
Subscripts	
e	electron
lim	limiting value
r	reactant
tot	total

increasing cell current density beyond ohmic region (linear trend) up to the maximum value allowed by diffusion limits without reaching a zero cell voltage, that is up to the limiting current density. Tests have been performed by separately varying the concentration of reactants (CO_2 or O_2 at the cathode and H_2 at the anode) with respect to a reference gas composition to identify the dependence of anodic as well as cathodic limiting current density on operating parameters.

The analysis of these experimental data requires particular attention because it is difficult to isolate the diffusion effects of each single reactant on voltage drop. In fact, although the size of the cell is small (about 55 cm^2), different parts of the cell may work under diffusion limiting conditions due to different reactants. The merging of these effects in overall voltage and current measurements complicates the identifying of separate anode and cathode limiting currents and cases can be isolated only when a sole reactant, under high dilution conditions, is limiting on the entire cell.

In this paper, we will present and discuss our experimental and theoretical work and underline the usefulness of the results for applications to stack and MCFC plant process design.

2. The kinetics model

This paper proposes an extension to a wider operating condition validity range of the electrochemical kinetics relationship

$$V = E - RJ \tag{1}$$

discussed in the previous paper [1].

In Eq. (1) a linear dependence of cell voltage V as a function of local current density J was assumed to calculate the losses reducing the thermodynamic voltage E. So, the electrochemical cell performance was evaluated on the basis of a local electrical resistance R, due to ohmic and different polarisation effects. In particular, R was written as the following semi-empirical relationship

$$R = \frac{A\mathrm{e}^{B/T}}{p_{O_2}^{\beta}} + s_{iR} + D\mathrm{e}^{G/T} \tag{2}$$

where p_{O_2} is the partial pressure of cathodic oxygen, T the solid temperature, s_{iR}, β, B, G, A and D are coefficients evaluated by experimental data (see also for numerical values [1]).

Using these electrochemical kinetics a good agreement was obtained for single cells as well as for cells assembled in stacks at different operating conditions. Nevertheless, considering the experimental results collected on cells operating at high current density or with poor reactant gases, a good agreement was only obtained by introducing a corrective coefficient in terms of a constant factor penalising performance at high utilisation factors [2].

The above consideration has suggested the need to investigate diffusion phenomena more deeply in a wider range of operating conditions and on the basis of a theoretical approach.

In particular, the voltage decay related to diffusion of each reactant, well known as concentration polarisation, can be written as follows [3]:

$$\eta_{r,conc} = \frac{R_g T}{n_r F} \ln\left(1 - \frac{J}{J_{r,lim}}\right) \tag{3}$$

where $J_{r,lim}$ is the limiting current density, that is, the maximum current reachable when the limiting reactant concentration on the electrode surface approaches zero.

Nevertheless, as the linear contribution of concentration polarisation has been already considered in parameter validation of resistance R (Eq. (2)), not to count this effect two times, only the non-linear part of Eq. (3) has been taken into account:

$$\eta_{r,conc,non\text{-}lin} = \frac{R_g T}{n_r F}\left[\ln\left(1 - \frac{J}{J_{r,lim}}\right) + \frac{J}{J_{r,lim}}\right] \tag{4}$$

In this way, the following cell voltage expression has been used:

$$V = E - RJ - \sum_r \eta_{r,conc,non\text{-}lin} \quad (5)$$

where $\eta_{r,conc,non\text{-}lin}$ is the non-linear part of the voltage decay related to diffusion of each reactant.

In conclusion, neglecting O_2 diffusion effect on the basis of experimental results (see Section 3), the electrochemical kinetics model proposed is the following:

$$V = E - \left(\frac{Ae^{B/T}}{p_{O_2}^{\beta}} + s_{iR} + De^{G/T}\right)J - \frac{R_g T}{n_r F}\left[\ln\left(1 - \frac{J}{J_{H_2,lim}}\right) + \frac{J}{J_{H_2,lim}} + \ln\left(1 - \frac{J}{J_{CO_2,lim}}\right) + \frac{J}{J_{CO_2,lim}}\right], \quad n_r = 2 \quad (6)$$

The limiting current densities can, on the basis of Faraday's and Fick's laws and neglecting effects of counter diffusion [4], be evaluated as follows:

$$J_{r,lim} = n_r F K_{Cr} c_r^b \quad (7)$$

if c_r^b is the reactant concentration in the bulk and K_{Cr} the mass transport coefficient.

So, in order to use the formulation (6), it is necessary to know the values of the mass transport coefficients K_{Cr}. They can be identified by standard experimental tests on an MCFC cell if correlated to an entity of easy evaluation such as the utilisation limiting factor $u_{r,lim}$, which has been defined as the ratio between the reactant flow rate consumed when limit operating condition extends all over the cell and the reactant flow rate fed to the cell.

In fact, starting from this definition and assuming to operate with diluted gases, the local value of molar fraction y_r can be written as a function of the local utilisation factor u_r as follows:

$$y_r = y_r^0(1 - u_r) \quad (8)$$

Then, the mass balance of the limiting reactant flowing along an electrode can be written in the following form (where l is the spatial coordinate with origin at gas flow inlet, see Fig. 1)

$$Q_r^0 \frac{du_r}{dl} = K_{Cr} c_r^b = K_{Cr} c_r^0 (1 - u_r) \quad (9)$$

with $u_r = 0$ for $l = 0$; $u_r = u_{r,lim}$ for $l = L$.

After integrating Eq. (9), K_{Cr} can be easily evaluated by $u_{r,lim}$ data as follows:

$$K_{Cr} = -\frac{Q_r^0}{L c_r^0} \ln(1 - u_{r,lim}) \quad (10)$$

In this way, thanks to a series of tests conducted until limit operation conditions, $u_{r,lim}$ and so K_{Cr} have been experimentally identified as discussed in the following section.

So, in comparison with previous approaches [5–9], more detailed but difficult to be experimentally validated, the above semi-empirical voltage decay expression (Eq. (6)) shows a complete phenomenological description with a minimum number of measurable parameters.

Integrating Eq. (6) into the macroscopic MCFC cell model, cell behaviour up to limiting diffusion operating conditions has been analysed and a good agreement between simulated and measured results has been obtained (see Section 4).

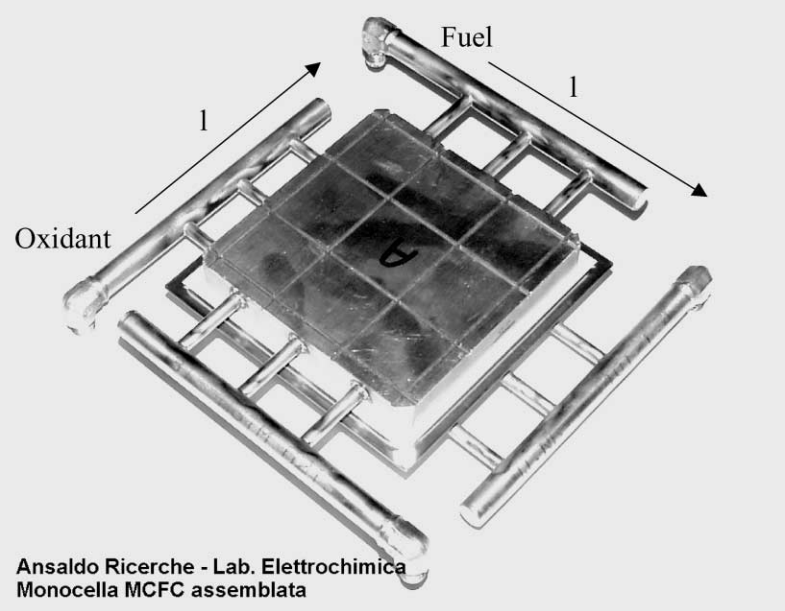

Fig. 1. Reactant feeding directions in the MCFC single cell used for tests.

3. Experimental

Experimental activity was carried out on an MCFC square planar single cell of about 55 cm^2 area, where the anode was a Ni/Cr alloyed powder, the cathode a lithiated nickel oxide structure and the electrolyte a lithium carbonate and potassium carbonate mixture [10]. The cell was tested in the experimental facility shown in Fig. 2, where the cell was held in a vessel and it was possible to set-up and control each operating parameter [11].

As above mentioned, a number of performance curves were carried out, increasing cell current density beyond ohmic region (linear trend) up to the maximum value allowed by diffusion limits without reaching a null cell voltage.

In particular, two series of tests were performed at 923 K, temperature kept constant on the cell plane using heating plates. A first one aimed at analysing effect of reactant diffusion by varying the concentration of H_2 with respect to the reference gas composition reported in Table 1 as ''Anode I'' coupled with a poor cathodic feeding (''Cathode IA'') as well as a rich cathodic feeding (''Cathode IB'').

In these tests H_2 molar fraction was changed from 0.06 up to 0.7 balancing this variation by reducing N_2, as it is an inert component, from 0.8 down to 0.16 in order to isolate the H_2 effect. Fig. 3 shows the related experimental characteristic curves obtained at atmospheric pressure using the ''IA'' composition at the cathode: the linear part of each curve is parallel to the other ones, according to the assumed independence of electrical resistance from H_2 concentration (see Eq. (2)). On the contrary, at high utilisation factor, performance decreases disclosing different limiting current densities for different H_2 concentrations.

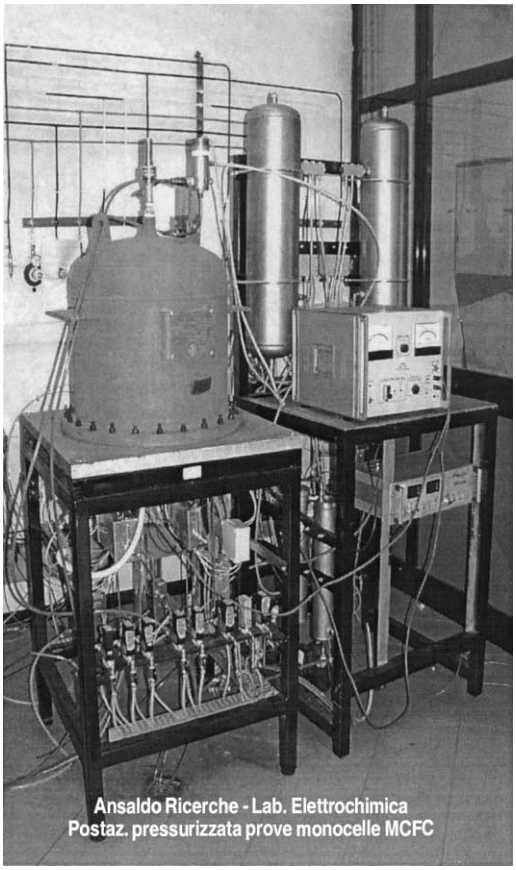

Fig. 2. MCFC single cell test facility.

Table 1
Reference gas compositions and flow rates (mol $s^{-1} \times 10^5$)

Operating conditions	CO_2	H_2	H_2O	N_2	O_2
Anode I	1.4	6.5	2.3	15.8	–
Cathode IA	14.3	–	–	125.0	15.1
Cathode IB	48.0	–	–	93.3	24.8
Anode II	2.4	36.6	3.8	–	–
Cathode II	23.3	–	–	205.4	24.8

With reference to Fig. 3, the current density values corresponding to the minimum voltage achieved along characteristic curves identify the best experimental evaluation of the limiting current densities. The latter are reported in Fig. 4 versus H_2 feeding molar fraction ($y^0_{H_2}$). The figure shows that for $y^0_{H_2}$ less than 0.15 the dependence of current density versus $y^0_{H_2}$ is linear as expected from the following overall cell balance

$$J_{r,lim} = \frac{n_r F Q^0_{tot} y^0_r (1 - u_{r,lim})}{L} \tag{11}$$

where

$$u_{r,lim} = 1 - \exp\left(-\frac{L c^0_r K_{Cr}}{Q^0_r}\right) = \text{constant} \tag{12}$$

as obtained from Eq. (10).

In this region, then, the cell seems working in only anodic limiting diffusion conditions: the H_2 limiting utilisation factor can so be experimentally identified as $u_{H_2,lim} = 0.75$

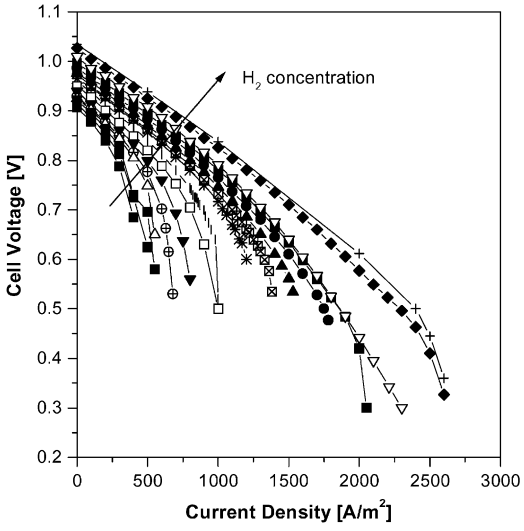

Fig. 3. Experimental characteristic curves at different inlet anodic H_2 molar fractions (at 650°C and 1 atm).

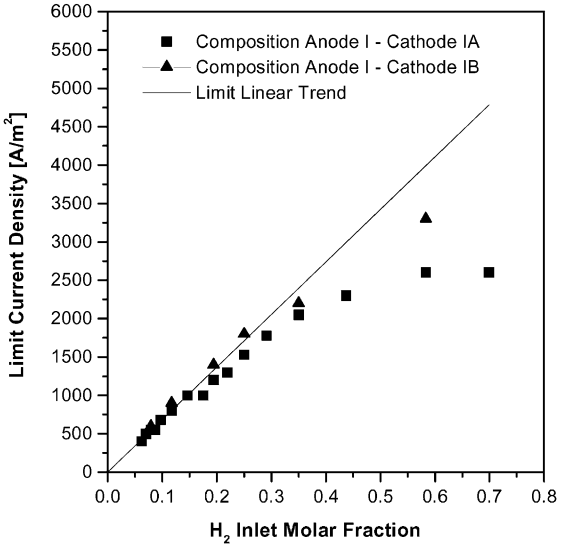

Fig. 4. Measured limit current density at different inlet anodic H_2 molar fractions (at 650°C and 1 atm).

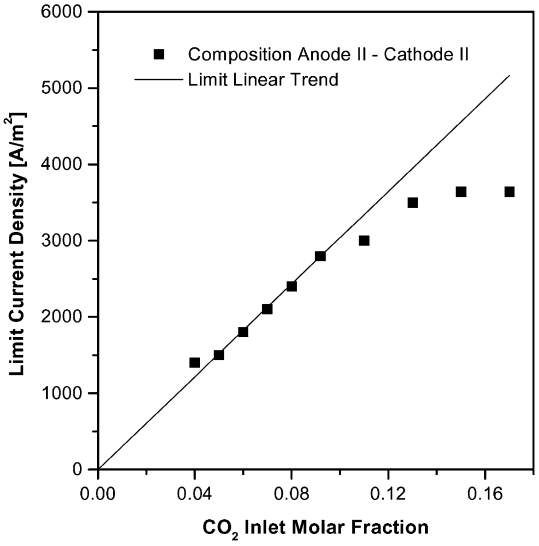

Fig. 5. Measured limit current density at different inlet cathodic CO_2 molar fractions (at 650°C and 1.5 atm).

and the related average mass transport coefficient is evaluated from Eq. (10) equal to $K_{C,H_2} = 0.011\,m\,s^{-1}$. This value is very low with respect to typical transport coefficients in the homogeneous gas phase on the electrode because it additionally contains the contribution of all transport and chemico-physical phenomena of the reactants (e.g. diffusion, solution, adsorption, ...) in the complex structure of the electrode.

For H_2 molar fraction higher than 0.15 the curve of Fig. 4 bends, because cathodic diffusion also becomes significant in this range. When CO_2 and O_2 utilisation factors achieve respectively 0.53 and 0.24, the limiting current density seems to become independent of H_2 concentration and to be bound only by cathodic gas diffusion. In order to verify this interpretation new tests have been performed with a richer cathodic composition (''Cathode IB''). The experimental results show that limiting current densities increase as expected (Fig. 4) and confirm that the previously observed flat behaviour is caused by cathodic limit conditions.

So, preliminary tests have been carried out to allow a qualitative analysis of the cathodic diffusion limits following the same procedure previously used for anodic tests.

In this case the two reactants (CO_2 and O_2) involved in the cathode reaction have to be considered. Operating conditions ''Anode II'' and ''Cathode II'' (Table 1) have been used as reference at anode and cathode side respectively, CO_2 and O_2 have been varied parametrically one by one.

During the first test, CO_2 molar fraction has been varied from 0.02 up to 0.15. After replacing reference conditions, the second test has been carried out changing O_2 molar fraction from 0.04 up to 0.16.

The results are reported in Figs. 5 and 6.

The curve versus $y^0_{CO_2}$ shows an experimental trend similar to the H_2 one: a first linear part and then a part independent of reactant concentration.

With regard to O_2, the characteristic curves have not been carried out up to limit operating conditions as advanced as for the previous tests, because low O_2 concentration sensibly penalises cell resistance (see Eq. (2)) and it would be necessary to reach a too low cell voltage.

Fig. 6 shows the maximum current densities achieved in these tests plot versus O_2 molar fraction. The curve does not show any dependence from O_2 molar fraction except at very low concentrations. Moreover, these concentrations are never used during cell standard operation, also because cell feeding is usually rich in air in order to optimise thermal management.

On the basis of this result, O_2 diffusion effects have been considered negligible and the decay of curve in Fig. 4 has

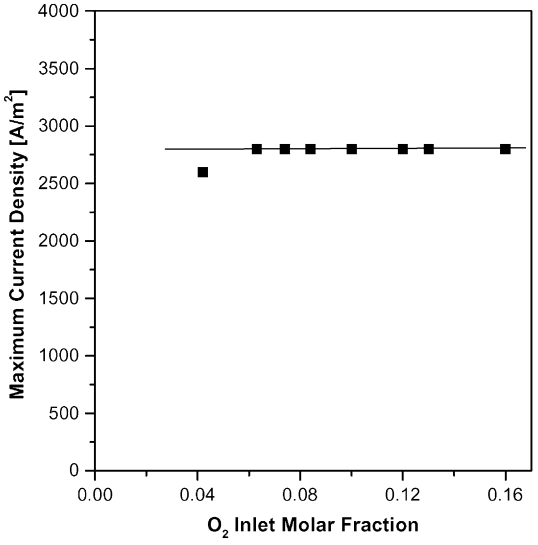

Fig. 6. Maximum measured current density at different inlet cathodic O_2 molar fractions (at 650°C and 1.5 atm).

been imputed to CO_2 diffusion. In this way the asymptotic trend of Fig. 4 has been used to identify the CO_2 utilisation factor about equal to 0.53 and so to calculate the average mass transport coefficient $K_{C,CO_2} = 0.035\,m\,s^{-1}$.

It is to be noted that our theoretical approach (Eq. (11)) refers to conditions where the diffusion of only one component (H_2 or CO_2) is limiting on all over the cell. On the contrary, our experimental values are believed to refer to limiting current conditions where one or more components are controlling (H_2 and/or CO_2). So, among these experimental points the ones belonging to proportional trends of current density versus reactant concentration are selected and compared to Eq. (10) in order to individuate the mass transport coefficients.

4. Model validation

First of all, we observed a systematic discrepancy in single-cell experimentation between experimental and theoretical open circuit voltages. In this case it has been taken into account within the model, lowering the Nernst value by 0.055 V in the local voltage calculation. This phenomenon is under study and is likely to be due to parasitic currents facilitated by single-cell assembling, in fact it is negligible in stacked cells. On the other hand, corrections up to 0.2 V are usual for other fuel cell types [12].

Then, thanks to the kinetics relationship previously discussed and integrated into the macroscopic MCFC cell model, a good agreement has been obtained between simulated and measured points. Fig. 7 shows, as an example, the results related to three performance curves: at high $y^0_{H_2}$ (0.58), when cathodic diffusion effects are prevailing, at average $y^0_{H_2}$ (0.22), when both anodic and cathodic diffusion

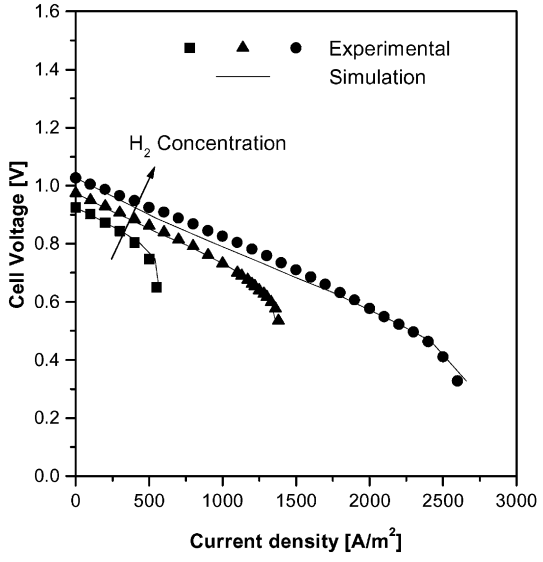

Fig. 7. Measured and calculated characteristic curves at different H_2 molar fractions ("Anode I" and "Cathode I").

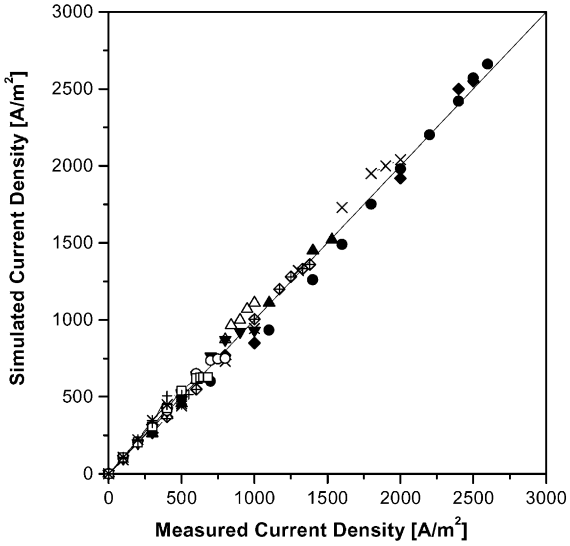

Fig. 8. Comparison between simulated and measured current densities at different operating conditions (indicated by different symbols).

phenomena are significant, and at low $y^0_{H_2}$ (0.08), when H_2 is the limiting reactant.

Then, the reliability of the model has been verified in the overall experimental range of H_2 concentration. Fig. 8 compares simulated and experimental current densities of the first test series in a parity plot always showing a satisfactory agreement. In particular, an average error less than 7% has been calculated, considering also data obtained in diffusion limit conditions. These results confirm the reliability of the theoretical approach of the model, while additional experimental tests are scheduled to estimate the mass transport coefficients more accurately in a wider range of operating conditions (compositions, temperature, pressure, specific flow rates, ...).

Figs. 9 and 10 show the calculated maps on the cell plane of the ratio $J/J_{r,lim}$ between local current density and anodic and cathodic limiting current density, respectively at the operating conditions reported below the figures.

These operating conditions correspond to a point belonging to the final linear trend of the second characteristic curve reported in Fig. 6. From the map analysis, it can be observed that, even if the cell is running under apparently safe conditions, parts of the cell work in diffusion limit operating conditions ($J/J_{r,lim} \rightarrow 1$). In addition, on the cell plane it is possible to detect contemporary an anodic diffusion control at the fuel outlet and a cathodic one at the cell corner where fuel is fresh and oxidant exhaust. The location of these regions depends on reactant concentration and local current density maps.

Moreover, it is interesting to observe that local diffusion limit conditions can be reached also when concentration polarization values are significantly lower than cell voltage. For example, in the case discussed above the local maximum η_{conc} on the cell plane is only 1/5 of cell voltage, but involves current density close to the limit value.

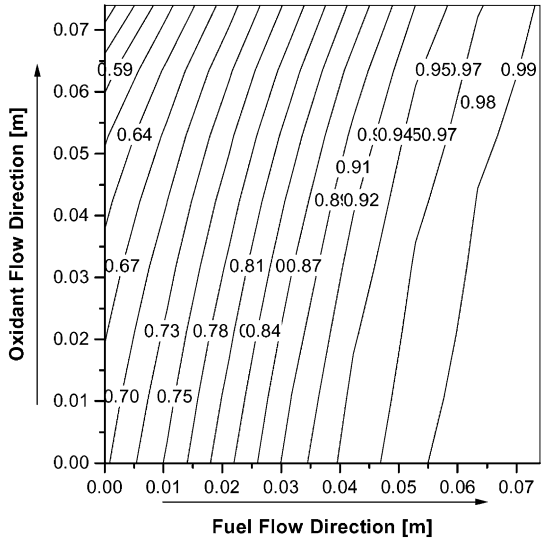

Fig. 9. Calculated map on the cell plane of the ratio between current density and anodic limit current density (Anode: CO_2 1.4×10^{-5} mol s^{-1}, H_2 9.1×10^{-5} mol s^{-1}, H_2O 2.3×10^{-5} mol s^{-1}, N_2 13.2×10^{-5} mol s^{-1}; Cathode: CO_2 14.3×10^{-5} mol s^{-1}, N_2 125×10^{-5} mol s^{-1}, O_2 15.1×10^{-5} mol s^{-1}; Cell voltage: 0.523 V).

The knowledge of $J/J_{r,lim}$ maps is important in choosing safe conditions available for the entire cell, in fact, standard working points showing local limiting diffusion conditions have to be avoided in order to preserve cell performance. This problem could be very significant when stacked cells are integrated in power plants with strong recycles that involve the feeding of diluted gases to the cells.

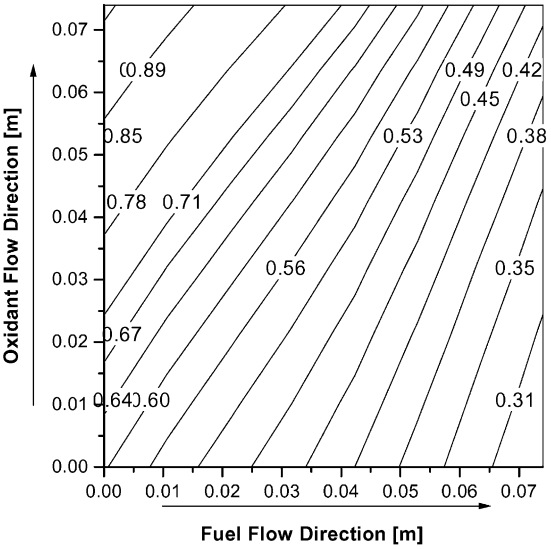

Fig. 10. Calculated map on the cell plane of the ratio between current density and cathodic limit current density (Anode: CO_2 1.4×10^{-5} mol s^{-1}, H_2 9.1×10^{-5} mol s^{-1}, H_2O 2.3×10^{-5} mol s^{-1}, N_2 13.2×10^{-5} mol s^{-1}; Cathode: CO_2 14.3×10^{-5} mol s^{-1}, N_2 125×10^{-5} mol s^{-1}, O_2 15.1×10^{-5} mol s^{-1}; Cell voltage: 0.523 V).

5. Conclusion

In this paper the limit performance of MCFC cells at high reactant utilisation factors have been studied. Characteristic curves beyond the linear ohmic region have been obtained by specific tests; experimental results have been analysed, detecting for reactants the maximum admissible utilisation factor and the average mass transport coefficients.

An original expression of voltage decay which considers the effects of the diffusion limit region has been set-up and then integrated into the MCFC cell model. This new kinetics relationship depends on concentration polarisation due to H_2 and CO_2, while O_2 diffusion effects have been considered negligible.

The model has been validated in a wide range of operating conditions, obtaining a good agreement with experimental data.

In particular, when cells work under apparently safe conditions, our model allows to individuate possible local running in diffusion limit conditions characterised by local electrical current close to the anodic or cathodic limit value, even if concentration polarisation is not necessarily a large fraction of the cell voltage.

So we underline as in defining the global strategies of cell control, where several constraints have to be observed at the same time to guarantee safe cell running, the correct evaluation of limiting diffusion conditions also has to be taken into account together with, for example, the estimate of local temperature peaks and high pressure drops [2].

Finally, additional experimental tests are scheduled to more accurately estimate the mass transport coefficients of the reactants, which takes into account the contribution of all transport and chemico-physical phenomena in the complex structure of electrodes.

Acknowledgements

The authors wish to thank Arturo Torazza and Paolo Capobianco for the availability of the Ansaldo Ricerche's test facilities and Stefano Dodera for his help in carrying out experimentation.

References

[1] B. Bosio, P. Costamagna, F. Parodi, Modeling and experimentation of molten carbonate fuel cell reactors in a scale-up process, Chem. Eng. Sci. 54 (1999) 2907–2916.

[2] E. Arato, B. Bosio, R. Massa, F. Parodi, Optimisation of the cell shape for industrial MCFC stacks, J. Power Sources 86 (1/2) (2000) 302–308.

[3] J.H. Hirschenhofer, D.B. Stauffer, R.R. Engleman, Fuel Cells: a Handbook (Rev. 3), DOE/METC-94/1006(DE94004072), US Department of Fossil Energy, Morgantown Energy Technology Center, Morgantown, WV, 1994.

[4] D. Pletcher, F.C. Walsh, Industrial Electrochemistry, 2nd Edition, Chapman & Hall, London, 1990.

[5] T.L. Wolf, G. Wilemski, Molten carbonate fuel cell performance model, J. Electrochem. Soc. 130 (1983) 48–55.
[6] C.Y. Yuh, J.R. Selman, Porous-electrode modeling of molten-carbonate fuel cell electrode, J. Electrochem. Soc. 143 (1992) 1373–1379.
[7] J.O'M. Bockris, S. Srinivasan, Fuel Cells: their Electrochemistry, McGraw-Hill, New York, 1969.
[8] P.S. Christensen, H. Livbjerg, A new model for gas diffusion electrodes. Application to molten carbonates fuel cells, Chem. Eng. Sci. 47 (1992) 2933–2938.
[9] J.A. Prins-Jansen, J.D. Fehribach, K. Hemmes, J.H.W. de Wit, A three-phase homogeneous model for porous electrodes in molten carbonate fuel cells, J. Electrochem. Soc. 143 (1996) 1617–1628.
[10] B. Bosio, Fuel cell technology development, Ph.D. dissertation, DIAM, University of Genoa, 1999.
[11] B. Bosio, E. Arato, P. Capobianco, Theoretical model and experimental validation of a pressurised molten carbonate fuel cell, in: Proceedings of the International Conference on Mass and Charge Transport in Inorganic Materials, Lido di Jesolo, Italy, 2000.
[12] P. Costamagna, Transport phenomena in polymeric membrane fuel cells, Chem. Eng. Sci. 56 (2001) 323.